MGS Science - MOC
Skip **Navigation**: Avoid going through Home page links and jump straight to ... A **line scan camera** incorporating both wide angle (140 degree) and narrow angle ...
mpfwww.jpl.nasa.gov/mgs/sci/details/moctext.html - 4k - Cached - Similar pages

[PDF] CHAPTER 3 PAVEMENT MANAGEMENT DATA
File Format: PDF/Adobe Acrobat - View as HTML
... global positioning system (GPS) receiver and an inertial **navigation** system capable ... consisting of a Bassler 2000-pixel digital **line-scan camera**, ...
pw.nashville.gov/IMS/Paving/Documents/Chapter_3.pdf - Similar pages

Unified force law for granular impact cratering : Article : Nature ...
... set by the 50 kHz frame rate of the **line-scan camera**. ..... ARTICLE **NAVIGATION** - This issue. Table of contents for this issue · Previous article ...
www.nature.com/nphys/journal/vaop/ncurrent/full/nphys583.html - Similar pages

The UK Industrial Vision Association (UKIVA) - Machine vision ...
Multipix Imaging Ltd: MultiPix announce the fastest **line scan camera** on the ..... has announced the launch of its new inertial **navigation** system (INS) ...
www.ukiva.org/news.shtml - 68k - Cached - Similar pages

Tisfoon Ulterior Systems - Portfolio - Raleigh, North Carolina - Home
Navigation. Database Development. BDE. SQL Server, XML .... The Hide profile was detected by a Dalsa **line scan camera** interfaced to a Bitflow Raptor frame ...
www.tisfoon.com/samples.htm - 34k - Cached - Similar pages

[PDF] PRACTICAL EXPERIENCES WITH FILMS, CAMERAS AND **NAVIGATION** SYSTEMS
File Format: PDF/Adobe Acrobat
Full survey GPS **navigation** systems are now the standard ..... This is a fast **line scan camera** which, although it produces a ...
www.blackwell-synergy.com/doi/pdf/10.1111/0031-868X.00111 - Similar pages

2. Explanatory Notes1
The survey used a differential GPS **navigation** system provided by RACAL Geodetic. .... using a digital imaging track system equipped with a **line-scan camera**. ...
www-odp.tamu.edu/publications/204_IR/chap_02/c2_.htm - 19k - Cached - Similar pages

Maine GeoLibrary Board - About Us
Skip First Level **Navigation** | Skip All **Navigation** ... An airborne remote sensing system - a **line scan camera** from Mika the ADS 40 and the LIDAR system, ...
www.maine.gov/geolib/2003/march19.htm - 35k - Cached - Similar pages

PCIe-1430
A tree for site **navigation** will open here if you enable JavaScript in your browser. ... from an area-scan camera and a **line-scan camera** at the same time. ...
www.graftek.com/pages/PCIe-1430.htm - 13k - Cached - Similar pages

Observational Evidence for an Active Surface Reservoir of Solid ...
Jump to: Page Content, Section **Navigation**, Site **Navigation**, Site Search, ... MOC is a **line-scan camera** that acquires images one line at a time (similar to ...
www.sciencemag.org/cgi/content/full/sci;294/5549/2146 - Similar pages

Previous 1 2 3 **4** 5 6 7 8 9 10 11 12 13 **Next**

THE PHOTOGRAMMETRIC RECORD

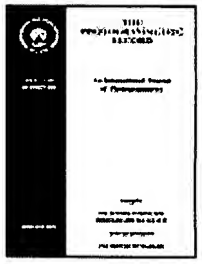

The Photogrammetric Record

Volume 16 Issue 91 Page 19 - April 1998

To cite this article: R. W. Graham, R. E. Read (1998)
Practical Experiences with Films, Cameras and Navigation Systems
The Photogrammetric Record 16 (91), 19–36.
doi:10.1111/0031-868X.00111

Prev Article | Next Article

Abstract

Practical Experiences with Films, Cameras and Navigation Systems

R. W. Graham & R. E. Read

[1]Aerial Imaging Systems Ltd.

Abstract

The first author commenced his experiences with aerial photography in 1945, when he joined the Royal Air Force (RAF). The aerial cameras used at that time were the Williamson F24 and F52, with Ilford HP3 and FP3 panchromatic films. Subsequently the Williamson F95 camera was tested against the USAF Sonne 11 camera. During his final years in the RAF, a variety of film types was employed: colour, monochrome infra-

red and false colour infra-red. Additional experience was gained when the author was employed by the International Training Centre (ITC), The Netherlands and he saw the further development of the air camera from the Wild RC8 and Zeiss (Oberkochen) RMK 15/23 to the Wild RC20, Zeiss (Jena) LMK and Zeiss (Oberkochen) RMK TOP. He predicts that the future lies with digital cameras.

The second author started working with aerial photography in the 1950s. Details are given of cameras, visual navigation sights and survey aircraft dating from that period. Overseas operations, carried out mainly by Hunting Surveys and Fairey Surveys, posed particular problems because the majority of the work there was undertaken without the aid of existing maps. The introduction of external navigation systems is described, from the Decca ship navigation system, through the GNS-200 VLF/Omega low frequency radio system to INS, the Inertial Navigation System. The author later joined the ITC, which enabled him to participate in trials of the Computer-controlled Photo Navigation System. Eventually practical experience was gained with differential GPS, particularly in countries in southeast Asia. Aerial photography currently appears to benefit less from financial investment than the photographic, aviation and survey industries. However, the satisfaction of making a significant contribution to major overseas development projects outweighs the frustration of lack of acceptance of plans for the future of the air survey industry.

IEEE Xplore® RELEASE 2.3

Results for "(navigation <and> (road <or> street) <and> (line scan camera) <in> pdfdata..." e-mail
Your search matched **6** of **1574558** documents.
A maximum of **100** results are displayed, **25** to a page, sorted by **Relevance** in **Descending** order.

» Search Options

View Session History

New Search

Modify Search

(navigation <and> (road <or> street) <and> (line scan camera) <in> pdfdata) <and> Search

Check to search only within this results set

Display Format: Citation Citation & Abstract

» Key

IEEE JNL	IEEE Journal or Magazine
IET JNL	IET Journal or Magazine
IEEE CNF	IEEE Conference Proceeding
IET CNF	IET Conference Proceeding
IEEE STD	IEEE Standard

view selected items Select All Deselect All

1. **IEEE IV2003 Intelligent Vehicles Symposium. Proceedings (Cat. No.03TH**
Intelligent Vehicles Symposium, 2003. Proceedings. IEEE
9-11 June 2003
Digital Object Identifier 10.1109/IVS.2003.1212870
AbstractPlus | Full Text: PDF(592 KB) IEEE CNF
Rights and Permissions

2. **Detection of street-parking vehicles using line scan camera and scanning sensor**
Hirahara, K.; Ikeuchi, K.;
Intelligent Vehicles Symposium, 2003. Proceedings. IEEE
9-11 June 2003 Page(s):656 - 661
Digital Object Identifier 10.1109/IVS.2003.1212990
AbstractPlus | Full Text: PDF(439 KB) IEEE CNF
Rights and Permissions

3. **The 29th Annual Conference of the Ieee Industrial Electronics Society**
Industrial Electronics Society, 2003. IECON '03. The 29th Annual Conference
Volume 2, 2-6 Nov. 2003 Page(s):i - xliv
Digital Object Identifier 10.1109/IECON.2003.1280184
AbstractPlus | Full Text: PDF(1809 KB) IEEE CNF
Rights and Permissions

4. **The 29th Annual Conference of the Ieee Industrial Electronics Society**
Industrial Electronics Society, 2003. IECON '03. The 29th Annual Conference
Volume 3, 2-6 Nov. 2003 Page(s):i - xliv
Digital Object Identifier 10.1109/IECON.2003.1280548
AbstractPlus | Full Text: PDF(1801 KB) IEEE CNF
Rights and Permissions

5. **IECON'03. 29th Annual Conference of the IEEE Industrial Electronics Soc No.03CH37468)**
Industrial Electronics Society, 2003. IECON '03. The 29th Annual Conference
Volume 1, 2-6 Nov. 2003
Digital Object Identifier 10.1109/IECON.2003.1279944
AbstractPlus | Full Text: PDF(2051 KB) IEEE CNF
Rights and Permissions

☐ **6. A fast stereo matching method for real time vehicle front perception with**
Hariti, M.; Ruichek, Y.; Koukam, A.;
Intelligent Vehicles Symposium, 2003. Proceedings. IEEE
9-11 June 2003 Page(s):247 - 252
Digital Object Identifier 10.1109/IVS.2003.1212917

AbstractPlus | Full Text: PDF(514 KB) **IEEE CNF**
Rights and Permissions

Refine Search

Search Results -

Terms	Documents
L11 and navigat$ and gps$	3

Database:
US Pre-Grant Publication Full-Text Database
US Patents Full-Text Database
US OCR Full-Text Database
EPO Abstracts Database
JPO Abstracts Database
Derwent World Patents Index
IBM Technical Disclosure Bulletins

Search: 10/719203

Refine Search

Recall Text Clear Interrupt

Search History

DATE: Thursday, May 24, 2007 Purge Queries Printable Copy Create Case

Set Name side by side	Query	Hit Count	Set Name result set
DB=PGPB,USPT,USOC,EPAB,JPAB,DWPI,TDBD; THES=ASSIGNEE; PLUR=YES; OP=OR			
L12	L11 and navigat$ and gps$	3	L12
L11	L4 and ((mobile$ or handheld or portable or moving) near3 (collect$ or record$)).clm.	481	L11
L10	l7 and L9	11	L10
L9	L8 and ((mobile$ or handheld or portable or moving) near3 (collect$ or record$))	11	L9
L8	L4 and navigat$ and gps$	126	L8
L7	L5 and navigat$ and gps$	11	L7
L6	L5 navigat$ and gps$	29031	L6
L5	L4 and ((mobile$ or handheld or portable or moving) near3 (collect$ or record$))	1636	L5
L4	l2 or L3	64434	L4

L3	(line$ with scan$ with (imag$ or camera)) and @pd<=20031121	46689	L3
L2	(line$ with scan$ with (imag$ or camera)) and @ad<=20031121	61178	L2

DB=PGPB,USPT; THES=ASSIGNEE; PLUR=YES; OP=OR

L1	20010056326 or 6473678.pn.	2	L1

END OF SEARCH HISTORY

RAPITRON

Technical notes
Line scan cameras

HOME PAGE ENGLISH
COMPANY PROFILE
HOT NEWS
OFFERS
INFO
MAILING LIST
SEARCH

PRODUCTS OVERVIEW
Security
Surveillance cameras
CCTV lenses
Digital Video Recorders
Monitors
IR lamps
Pan & tilts
Housings
Machine vision
Industrial cameras
Frame grabbers
Machine vision lenses
Lighting for machine vision
Accessories
Video transmission and networking
Video signal

What is a line scan camera?

A line scan camera is an image capturing device having a CCD sensor which is formed by a single line of photosensitive elements (pixels). Therefore, unlike area sensors which generate frames, in this case the image acquisition is made line by line.

One single scanning line of a line scan device can be considered as a one-dimensional mapping of the brightness related to every single point of an observed line. A linear scanning generates a line, showing on the Y axis the brightness of each point given in grey levels (from 0 to 255 levels).

A sudden change of the grey level in a single point corresponds either to a point on the edge of an object or to any colour or aspect variation of the acquired image. Detection of this change allows a precision measurement, thanks also to the high resolution on the linear sensor which is considerably better than the resolution of an area imager.

For instance, by using a backlight you may know the position and width of a strip, by observing the transition of every single point; or detect the impurities (holes, scratches, spots etc.) on any inspected surface.

For this type of camera the use of **lenses for line scan cameras** are recommended.

control devices

Printers

DISCONTINUED PRODUCTS

TECHNICAL NOTES

Optical calculator

Cliccate sulle parole evidenziate in **giallo** per vedere collegamenti a figure o ad altre pagine.
Click on words highlighted in yellow to view **links**.

Cliccate sulle immagini miniaturizzate per vederle ingrandite.
Click on thumbnails to view enlarged images.

Via Washington 59 - 20146 Milano ITALIA Tel.: +39 02 659.82.82 Fax: +39 02 65.45.25

P.IVA/VAT No: IT 04498890153

Title:

Computerized flight inspection system

Document Type and Number:
United States Patent 4792904
Link to this page:
http://www.freepatentsonline.com/4792904.html

Abstract:

A computerized flight inspection system is disclosed. The system of the present invention may be utilized to generate an accurate reference location with respect to an airport runway for an aircraft having an inertial navigation system. A selected geometric pattern having a highly unambiguous autocorrelation function is placed on at least one end of the runway. A video line scanning camera mounted to the aircraft is then utilized to scan the geometric pattern in a line generally perpendicular to the line of flight. The output of the video line scanning camera is then correlated with a stored reference pattern to generate a signal indicative of the detection of the geometric pattern on the runway. A laser altimeter is mounted to the aircraft and utilized to generate an accurate signal indicative of the aircraft altitude with respect to the runway pattern. The outputs of the correlation circuit and the laser altimeter are then utilized to correct data from the inertial navigation system.

Inventors:

Reinagel, Frederick G. (Buffalo, NY, US)
Johnson, Allen B. (North Tonawana, NY, US)

Application Number:

140875

Filing Date:

01/06/1988

Publication Date:

12/20/1988

View Patent Images:

Images are available in PDF form when logged in. To view PDFs, I

Referenced by:

View patents that cite this patent

Export Citation:

Click for automatic bibliography generation

Assignee:

LTV Aerospace and Defense Company (Dallas, TX)

Primary Class:

701/17

Other Classes:

73/178T, 340/953, 348/116, 348/117, 701/16, 702/94

Field of Search:

364/428-430, 439, 443, 456, 571 358/103 340/947, 948, 951, 953, 954, 955, 956 73/178 T

US Patent References:

4144571	Mar, 1979	Webber	364/429.
4210930	Jul, 1980	Henry	358/103.
4385354	May, 1983	Hornfeld et al.	340/953.
4534000	Aug, 1985	Bliss	364/429.
4584646	Apr, 1986	Chan et al.	364/443.

Primary Examiner:

Chin, Gary

Attorney, Agent or Firm:

Brooks & Kushman

Parent Case Data:

This is a continuation-in-part of co-pending application Ser. No. 065,075, filed on 6-17-87, abandoned, which is a continuation-in-part of application Ser. No. 946,124, filed 12-24-86, abandoned, which is a continuation-in-part of the present application Ser. No. 699,333 filed 2-7-85, abandoned.

Claims:

What is claimed is:

1. A computerized flight inspection system for providing an accurate reference location with respect to a runway for an aircraft having an inertial navigation system, said flight inspection system comprising:

selected indicia disposed on at least one end of an airport runway;

video scanning means disposed within said aircraft for scanning said selected indicia in a line generally perpendicular to said aircraft's line of flight and for generating an output indicative of the scanned video pattern;

memory means for storing a reference video pattern;

correlator means coupled to said video scanning means and said memory means for correlating said scanned video pattern and said reference video pattern;

altimeter means for measuring the altitude of said aircraft and for generating a signal indicative thereof; and

processor means coupled to said correlator means and said altimeter means for generating correction data for said inertial navigation system in response to said correlation and said altitude measurement.

2. The computerized flight inspection system according to claim 1 wherein said selected indicia comprises a selected geometric pattern.

3. The computerized flight inspection system according to claim 1 wherein said video scanning means comprises a solid state line scan camera.

4. The computerized flight inspection system according to claim 3 wherein said solid state line scan camera includes a charge couple device line scan image sensor.

5. The computerized flight inspection system according to claim 4 wherein said charge couple device line scan image sensor includes a single row of 1,024 image sensing elements.

6. The computerized flight inspection system according to claim 1 wherein said correlator means comprises a sixty-four bit monolithic digital correlator.

7. The computerized flight inspection system according to claim 1 wherein said altimeter means comprises a laser altimeter.

8. The computerized flight inspection system according to claim 1 wherein said processor means comprises an appropriately programmed microprocessor.

9. The computerized flight inspection system according to claim 1 wherein said memory means comprises a parallel-in-serial-out shift register.

10. The computerized flight inspection system according to claim 1 wherein said selected indicia disposed on at least one end of an airport runway comprises two identical indicia disposed on opposite ends of an airport runway.

11. A computerized flight inspection system for providing an accurate reference location with respect to a runway for an aircraft having an inertial navigation system, said flight inspection system comprising:

selected indicia disposed on at least one end of an airport runway;

video scanning means disposed within said aircraft for scanning said selected indicia in a line generally perpendicular to said aircraft's line of flight and for generating an output indicative of the scanned video pattern;

inertial navigation means for generating a plurality of signals indicative of aircraft position and attitude;

memory means for storing a reference video pattern;

correlator means coupled to said video scanning means and said memory means for correlating said scanned video pattern and said reference video pattern;

altimeter means for measuring the altitude of said aircraft and for generating a signal indicative thereof; and

processor means coupled to said inertial navigation system, said memory means, said correlator means and said altimeter means for modifying said reference video pattern in response to said plurality of signals indicative of aircraft position and attitude and said altitude signal; and for generating correction data for said inertial navigation means in response to the altitude and attitude of said aircraft and the output of said correlator means.

12. The computerized flight inspection system according to claim 11 wherein said selected indicia comprises a selected geometric pattern.

13. The computerized flight inspection system according to claim 11 wherein said video scanning means comprises a solid state line scan camera.

14. The computerized flight inspection system according to claim 13 wherein said solid state line scan camera includes a charge couple device line scan image sensor.

15. The computerized flight inspection system according to claim 14 wherein said charge couple device line scan image sensor

includes a single row of 1,024 image sensing elements.

16. The computerized flight inspection system according to claim 11 wherein said correlator means comprises a sixty-four bit monolithic digital correlator.

17. The computerized flight inspection system according to claim 11 wherein said altimeter means comprises a laser altimeter.

18. The computerized flight inspection system according to claim 11 wherein said processor means comprises an appropriately programmed microprocessor.

19. The computerized flight inspection system according to claim 11 wherein said memory means comprises a parallel-in-serial-out shift register.

20. The computerized flight inspection system according to claim 11 wherein said selected indicia disposed on at least one end of an airport runway comprises two mirror image indicia disposed on opposite ends of an airport runway.

Description:

BACKGROUND OF THE INVENTION

The present invention relates in general to aircraft navigation systems and in particular to systems for generating an accurate reference location with a respect to a runway. Still more particularly, the present invention relates to systems for generating position correction signals from optical observation for utilization in the inspection of instrument landing systems.

Instrument landing systems are well known in the prior art. Such systems can be utilized to permit appropriately equipped aircraft to land on airport runways under highly hazardous conditions. However, in order to utilize such systems it is necessary to periodically inspect and calibrate these systems to ensure that the electronic indications of aircraft location are sufficiently accurate with respect to actual aircraft location.

Highly accurate inertial navigation systems are known which generate relatively accurate indications of aircraft location from a selected point; however, these systems are not sufficiently accurate to permit the evaluation of Instrument Landing Systems (ILS). Thus, a more accurate method of generating aircraft location must be utilized.

In order to generate highly accurate reference locations of inspection aircraft, prior art systems have utilized a variety of approaches. For example, one system utilizes a ground-based optical tracking device such as a theodolite to generate a reference

location which may be compared to the electronically generated location provided by the instrument landing system. Other systems utilize ground-based optical reflectors which can be utilized to allow an aircraft equipped with light sources and detectors to obtain a reference location.

All such known systems require extensive groundbased equipment and/or operators to generate a reference location of the inspection aircraft. As such, some of these systems are subject to human error and some can only be operated during daylight hours in acceptable weather conditions. Thus, it should be apparent that a need exists for a flight inspection system which does not require extensive ground-based equipment or personnel and which generates a highly accurate reference location with respect to an airport runway.

SUMMARY OF THE INVENTION

It is therefore one object of the present invention to provide an improved flight inspection system.

It is another object of the present invention to provide an improved flight inspection system which does not require extensive ground-based equipment.

It is yet another object of the present invention to provide an improved flight inspection system which does not require ground-based support personnel.

It is still another object of the present invention to provide an improved flight inspection system which utilizes optical observations to generate position correction signals for utilization in the inspection of instrument landing systems.

The foregoing objects are achieved as is now described. A selected geometric pattern having a highly unambiguous autocorrelation function is placed on at least one end of an airport runway. A video line scanning camera mounted to the aircraft is then utilized to scan the geometric pattern in a line generally perpendicular to the line of flight. The output of the video line scanning camera is then correlated with a stored reference pattern to generate a signal indicative of the detection of the geometric pattern on the runway. A laser altimeter is mounted to the aircraft and utilized to generate an accurate signal indicative of the aircraft altitude with respect to the runway pattern.

The outputs of the correlation circuit and the laser altimeter are then utilized to correct data from the inertial navigation system.

BRIEF DESCRIPTION OF THE DRAWINGS

The novel features believed characteristic of the invention are set forth in the appended claims. The invention itself; however, as well as a preferred mode of use, further objects and advantages thereof, will best be understood by reference to the following detailed description of an illustrative embodiment when read in conjunction with the accompanying drawings, wherein:

FIG. 1 is a perspective view of an airport runway equipped with the novel flight inspection feature of the present invention;

FIG. 2 is a side view of an aircraft equipped with the novel flight inspection system of the present invention;

FIG. 3 is a plan view of a runway pattern which may be utilized with the novel flight inspection system of the present invention;

FIG. 4 is a diagram of the autocorrelation function of the runway pattern depicted in FIG. 3;

FIG. 5 is a block diagram of the novel flight inspection system of the present invention;

FIG. 6 is a block diagram of the video position references system of the novel flight inspection system of the present invention;

FIG. 7 is a more detailed block diagram of the video position reference system of the novel flight inspection system of the present invention;

FIG. 8 is a diagrammatic end view of an aircraft and runway having the runway pattern depicted in FIG. 3;

FIG. 9 is a diagrammatic side view of an aircraft and runway having the runway pattern depicted in FIG. 3; and

FIG. 10 is a flow chart illustrating the steps for using the optical pattern recognition system position coordinates to update an inertial navigation system error estimate.

DETAILED DESCRIPTION OF THE PREFERRED EMBODIMENT

With reference now to the figures and in particular with reference to FIG. 1 there is depicted a perspective view of an airport runway equipped with the novel flight inspection feature of the present invention. As can be seen, runway 10 is depicted as having a geometric pattern 12 disposed on each end thereof. As will be explained in greater detail herein, geometric pattern 12 is selected to have a highly unambiguous autocorrelation function and must be positioned across runway 10 with an accuracy of 0.5 inch for Category III system inspections. Geometric pattern 12 is preferably

located at the extreme ends of runway 10 to reduce wear due to aircraft wheel marks and exhaust gases. Geometric pattern 12 must not be obscured by dust, sand or snow in order to operate the system of the present invention; however, geometric pattern 12 is preferably approximately six feet wide and eighteen feet long and thus the area to be kept clear is quite small. Additionally, because of the nature of the autocorrelation operation, the system is tolerant to a considerable degree of pattern degradation.

Aircraft 14 is utilized to fly over geometric pattern 12 to obtain accurate reference position data. Preferably, the novel system of the present invention is initiated as aircraft 14 enters Instrument Landing System (ILS) envelope 16 by middle marker 18. Also depicted is inner marker 20, as those skilled in the art will appreciate.

Referring now to FIG. 2, there is depicted a side view of an aircraft 14 which illustrates certain features of the novel flight inspection system of the present invention. As can be seen, as aircraft 14 passes over runway 10 at an altitude of approximately thirty-five to seventy feet, a laser altimeter 22 is utilized to measure the altitude of aircraft 14. Those skilled in the art will appreciate that such laser altimeters are readily available in the industry and will provide altitude accuracy within a few inches. Laser altimeter 22 is utilized as an input to the positiondetermining computations of the present invention. Also depicted in FIG. 2 is digital scanning camera 24 which is utilized to scan geometric pattern 12 to provide reference position data as will be explained herein. As an installation consideration, scanning camera 24 should be positioned as closely spaced as possible to aircraft 14's inertial navigation system. As will be explained herein, roll, pitch and yaw information from the inertial navigation system will be utilized to correct the output of line scanning camera 24 and such an installation will reduce errors due to fuselage deflections.

With reference now to FIG. 3, there is depicted a plan view of geometric pattern 12 as installed on runway 10. While a specific pattern is depicted, the particular pattern selected is merely one of many patterns which exhibit a highly unambiguous autocorrelation function. The pattern depicted is constructed utilizing bright white bands 26, 28, 30 and 32, which are separated by black bands 34, 36 and 38. In the particular pattern depicted, band 26 is three units wide, band 28 is one unit wide and bands 30 and 32 are each two units wide. Similarly, black band 34 is two units wide and bands 36 and 38 are each one unit wide. It should also be noted that the aforementioned bands are not bounded by straight lines, but rather three separate contiguous segments of straight lines which change their rate of convergence at intersecting lines 40 and 42 to approximate an exponential function.

Referring now to FIG. 4, there is depicted a diagram of the

autocorrelation function of geometric pattern 12 of FIG. 3. As can be seen, peak 44 of the autocorrelation function is almost twice as great in magnitude than all remaining peaks in the autocorrelation function. In this manner, a reference pattern for geometric pattern 12 can be correlated with a scan across pattern 12 which is generally parallel to lines 40 and 42 and the resultant correlation function will indicate with a high degree of lateral resolution and certainty when a "match" has occurred.

With reference now to FIG. 5, there is depicted a block diagram of the novel flight inspection system of the present invention. As can be seen, the flight inspection system is controlled by central processor 46. Central processor 46 is preferably a suitably programmed single-band computer, such as the model HK-68-3, manufactured by Heurikon Corporation of Madison, Wis.

Coupled to central processor 46 are laser altimeter 22 and precision distance measuring equipment (DME) 48 which are utilized by central processor 46, together with the output of video position reference system 52 to generate an accurate position with respect to runway 10 which may be utilized to correct Inertial Navigation System (INS) 50 for position offset and drift. In this manner, aircraft position data generated by INS 50 is thus made sufficiently accurate to permit evaluation of Category III Instrument.

In a preferred mode of the present invention, INS 50 is preferably a Delco Carousel IV Inertial Navigation System. The Delco Carousel IV INS provides approximately an order of magnitude of improvement over conventional INS systems with regard to zero offset of the "x" axis and the "y" axis accelerameters. Also coupled to central processor 46 are strip chart recorder 58 and display 60. Strip chart recorder 58 may be implemented utilizing any suitable recorder and may be utilized to provide complete recording of each test flight.

The use of a wide range of avionics equipment 62 is accommodated with this preferred mode of the present invention. Test receivers/transmitters for the checking of ILS (Instrument Landing Systems), VOR (VHF Omnidirection Range), TACAN, MKR (Marker Beacons), and communication equipment are connected to an Inspection Data Acquisition subsystem 56 containing suitable translation interfaces and a slave microprocessor which organizes, formats and controls the data for subsequent use by the central processor 46.

All avionics data received by the central processor, plus positional data computed thereby, are available for recording on a magnetics tape unit 54 for long-term storage. These data are also available for visual presentation on the CRT display unit 60 or strip chart recorder 58.

Referring now to FIG. 6, there is depicted a block diagram of video position reference system 52 of FIG. 5. As can be seen video signals indicative of the scanned pattern are generated by line scanning camera 24. These signals are then processed by video processor 64. Video processor 64 is utilized to produce a quantized serial data stream having a bit state indicative of the detection of "black" or "white" by digital line scanning camera 24.

The serial data stream from video processor 64 are then coupled to correlator 66 and compared to a stored reference pattern therein. In a preferred mode of the present invention, correlator 66 is provided by a monolithic 64 bit digital correlator such as the TDC 1023J, manufactured by TRW, Inc. of Redondo Beach, Calif. A correlation score is generated for each comparison and that correlation score is then compared to the highest correlation score previously obtained and stored in digital peak detector 68. If the current correlation score is higher than the score stored in digital peak detector 68, the new score is stored within digital peak detector 68 and strobe signals are generated which update the data in both cross-track register 70 and scan number register 72.

As each strobe signal is coupled to cross-track register 70, that register stores the pixel count generated by timing generator 74. Timing generator 74 generates a pixel count beginning with zero at the beginning of each scan of digital line scanning camera 24. Thus, the value stored in cross-track register 70 will correspond to the lateral position of the runway reference pattern within each scan of digital scanning camera 24.

Similarly, scan number register 72 acquires and holds the number of the scan during which the maximum correlation score occurs. The scan register is generated by timing generator 74 and is set to zero each time central processor 46 reads a frame of data, and advances at the scan rate. In a preferred embodiment of the present invention, the scan rate is preferably 200 scans per second. Additionally, digital peak detector 68 is also reset to zero at the beginning of each data frame.

The occurrence of the runway pattern detection is selectively defined as the highest correlation score above some predetermined threshold value. For example, a correlation score of 56 or more bit matches out of 64. Such a threshold will be high enough to discriminate against random background image patterns and will also tolerate some degree of reference pattern degradation. An event detection permits the pattern lateral position (determined by the contents of cross-track register 70) and the time of occurrence (determined by the content of scan number register 72) to be combined by central processor 46 with aircraft altitude (as detected by laser altimeter 22) and aircraft attitude (as detected by Inertial Navigation System 50) to compute the actual position of the aircraft relative to runway 10 with a precision sufficient for

instrument landing system inspection.

With reference now to FIGS. 8 and 9 an aircraft and runway having the reference pattern template of the present invention is depicted to explain the computation of aircraft position relative to the runway. The position of the flight-inspection aircraft is defined with respect to a reference point on the runway where the centerline of the runway intersects the threshold line. The position of the aircraft is described in Cartesian coordinates as follows:

x=displacement from the centerline;

y=displacement from the threshold along the centerline;

z=altitude above the runway surface.

The runway surface is assumed for calculations to be essentially flat and level. During flight inspection path profiles the aircraft pitch angle is relatively small, less than 60 and the aircraft roll angle is also relatively small, less than 10.degree.. Therefore, secondorder coupling terms are negligibly small. By applying small-angle approximations, the altitude above the runway, with precision sufficient for instrument landing system inspection, is given by:

z=r cos (.alpha..sup.2 +.beta..sup.2).sup.1/2

where:

r=range to the runway surface measured by the laser altimeter;

.alpha.=aircraft roll angle;

.beta.=aircraft pitch angle.

By applying small-angle approximations, the x and y components of the aircraft position are independently derived. Referring to FIG. 8, the value of the cross-track component x is determined by the position of the reference pattern image on the photosensitive array of the line-scan camera, the aircraft roll angle and the aircraft altitude as given by the following equation:

x=z (tan .alpha.-.DELTA./f) where:

z=true altitude above the runway;

.alpha.=aircraft roll angle;

.DELTA.=displacement of the referenced pattern centerline image from the optic axis;

f=focal length of the camera lens.

The distance .DELTA. is measured by multiplying the difference between the time intervals from the start of a line scan to the occurrence of the correlation peak, and that which corresponds to the reference pattern centerline image coinciding with the optic axis, by the line scan rate.

The on-track component y of the aircraft position is measured by first determining from the laser altimeter slant range and camera optics, the point P on the runway reference pattern where the size of its image on the camera's line array equals that of the correlator's reference pattern (see FIG. 3). At the instant the maximum correlation occurs, the aircraft on-track position may be understood by reference to FIG. 9 and the following equation:

y=y.sub.1 +z tan .beta.

where:

y=aircraft distance to the shortest threshold point;

y.sub.1 =distance from P to the threshold point;

z=true altitude above runway;

.beta.=aircraft pitch angle.

In the illustrated case, the pitch angle is negative as is typical with actual flight inspection paths. Thus, the term z tan .beta. is also negative which results in y being smaller than y.sub.1.

FIG. 10 illustrates the use of the optical pattern recognition system to update an inertial navigation system error state estimate based upon the precision position calculations of the optical pattern recognition system.

FIG. 10 is a flow chart of the processing utilized to perform an update in a conventional Kalman Filter. The optical pattern recognition system 102 (OPRS) provides the coordinates (x,y,z) where x is distance across runway centerline, y is distance along runway centerline and z is vertical. A standard coordinate conversion 104, in this case a simple rotation, converts these runway coordinates into precise east, north, and vertical coordinates (E, N, Z) .sub.REF of the aircraft at the instant of pattern passage.

The INS 106 provides time tagged latitude (.phi.), longitude (.lambda.) and altitude (Z) which are interpolated to obtain the INS measured position at the time of pattern overflight. These geodetic coordinates are converted 108 into East, North and vertical

coordinates (E, N, Z) .sub.INS with respect to the plane tangent to the earth at runway pattern. Standard geodetic to planar coordinate conversions which account for the ellipticity of the earth are used for this step.

At this point in the processing 110, we have two opinions of the position of the aircraft at the instant of pattern overflight, from the INS and the OPRS. The error in the INS measured position is typically on the order of hundreds of feet. The OPRS error is on the order of inches. The precision position obtained at each overflight of the runway pattern is used to make an update in the classic Kalman Filter sense of the estimate of the errors in the Inertial Navigation System (INS). The simple algebraic difference between the two is an excellent estimate of the INS error for that instant of time.

Therefore, this difference is used as the measurement vector in the standard Kalman Filter 112 on the error in the INS. In the Kalman Filter, the error state vector 114 is the estimate of the INS error states as to position, velocity, gyro drift rates, accelerometer biases, and mislevel. This error state vector is time varying and as a result, a time sequence of OPRS updates will provide increasingly improved estimates of the states representing higher derivatives. The first pass provides excellent position, the second pass provides velocity and so on.

These INS error state estimates are then used by the flight inspection computer to correct the INS measurements made from the Outer Marker down to the runway. These corrected INS measurements are used in turn as the reference for determination of the localizer and glidepath error in the Instrument Landing System being inspected.

Also included in FIG. 6 is illumination system 76 which may be utilized to illuminate runway 10 and pattern 12 so that flight inspection can be accomplished during night hours. It should also be noted that in view of the fact that pattern 12 is not symmetrical, it will be necessary to provide an inbound/outbound signal to correlator 66 so that the reference pattern template may be reversed to detect pattern 12.

With reference now to FIG. 7, there is depicted a more detailed block diagram of the video position reference system of FIG. 5. As can be seen, digital line scanning camera 24 produces, in the depicted embodiment, two output video channels 76 and 78. In a preferred embodiment of the present invention, digital scanning camera 24 is implemented utilizing an industrial line scan camera such as the Model CCD 1300R manufactured by Fairchild Camera and Instrument Corporation of Palo Alto, Calif. This particular model utilizes CCD imaging techniques and puts out two time division multiplex video outputs.

In order to extract the essential features of geometric pattern 12 over a wide range of absolute image brightness, analog video outputs 76 and 78 are coupled into a pair of wide-band logarithmic response amplifiers 84 and 86. In a preferred embodiment of the present invention an independent auto-biasing circuit is utilized in conjunction with each logarithmic response amplifier to establish a precise black level operating point. This is achieved by activating the sample state of sample-and-hold circuits 80 and 82 at a pixel count which coincides with the black reference video output level.

The outputs of logarithmic response amplifiers 84 and 86 are then coupled to linear difference amplifier 88. Those ordinarily skilled in the art will appreciate that the well known mathematical properties of logarithms will result in the output of difference amplifier 88 being a constant value for sets of video input signals having a constant ratio, regardless of absolute value. Since the two video channel odd/even format produces light intensity levels of adjacent pixels simultaneously, the difference amplifier output indicates the ratio of light intensity change between adjacent pixels. However, a polarity reversal is introduced each pixel period because of the alternating sign of the most recent data.

Although a sharp black-to-white or white-to-black transition is the video feature being sought, allowance must be made for the possibility of the edge of geometric pattern 12 falling in the center of a pixel sensing element producing an intermediate average intensity. For this reason, the ratio threshold value must be set at somewhat less than a ratio of two-to-one to ensure adequate probability of detection. Voltages corresponding to the threshold ratio and its reciprocal are supplied to a pair of analog comparator amplifiers 90 and 92 which are coupled to the output of high pass filter 94. The outputs of analog comparator amplifiers 90 and 92 are then decommutated on an odd/even basis utilizing switch 96. The resultant ouptut enables the setting and clearing of bistable multivibrator 98 which produces a one-bit quantized video output which is required by digital correlator 66. In the depicted mode of the present invention, the state of that bit will be zero for a black detection and one for a white detection.

As explained above, a digital reference pattern is stored within reference pattern register 100 and then correlated with the digitized output of a line scanning camera to determine the detection of geometric pattern 12. Digital peak detector 68 is implemented utilizing a seven-bit latch and is updated each time the output of correlator 66 is greater than a previous output. Oscillator 74 is utilized to generate timing pulses, and cross-track register 70 and scan number register 72 are implemented utilizing an eleven-bit latch and a four-bit latch respectively. Eleven-bit counter 71 is utilized in conjunction with cross-track register 70 and four-bit counter 73 is utilized in conjunction with scan number register 72.

Those ordinarily skilled in the art will appreciate upon reference to the foregoing specification that when utilizing the video position reference system of the present invention of an inspection aircraft may fly over an airport runway and utilize visual information to obtain a substantially exact reference position of the aircraft with respect to the runway which may then be utilized to upgrade the onboard inertial navigation system to an accuracy sufficient to permit Class III instrument landing systems to be calibrated.

Although the invention has been described with reference to a specific embodiment, this description is not meant to be construed in a limiting sense. Various modifications of the disclosed embodiment as well as alternate embodiments of the invention will become apparent to persons skilled in the art upon reference to the description of the invention. It is therefore contemplated that the appended claims will cover any such modifications or embodiments that fall within the true scope of the invention.

<- Previous Patent (Microprocessor controlled post ejec...) | Next Patent (Method of fuel injection control in...) ->

Science 7 December 2001:
Vol. 294. no. 5549, pp. 2146 - 2148
DOI: 10.1126/science.1066416

REPORTS

Observational Evidence for an Active Surface Reservoir of Solid Carbon Dioxide on Mars

Michael C. Malin,* Michael A. Caplinger, Scott D. Davis

High-resolution images of the south polar residual cap of Mars acquired in 1999 and 2001 show changes in the configuration of pits, intervening ridges, and isolated mounds. Escarpments have retreated 1 to 3 meters in 1 martian year, changes that are an order of magnitude larger than can be explained by the sublimation of water ice, but close to what is expected for sublimation of carbon dioxide ice. These observations support a 35-year-old conjecture that Mars has a large surface reservoir of solid carbon dioxide. The erosion implies that this reservoir is not in equilibrium with the present environment and that global climate change is occurring on Mars.

Malin Space Science Systems, Post Office Box 910148, San Diego, CA 92191-0148, USA.
* To whom correspondence should be addressed.

In their seminal 1966 paper on the behavior of CO_2 and other volatiles on Mars, Leighton and Murray (1) deduced from a numerical thermal model that the polar caps are composed of frozen CO_2. They drew three other important conclusions from this analysis: (i) The year-round presence of solid CO_2 regulates the pressure of the atmosphere. (ii) The atmospheric pressure changes cyclically on a semiannual basis because of formation and retreat of the seasonal frost caps. (iii) The total amount of CO_2 on Mars could greatly exceed that presently in the atmosphere and form a large surface reservoir. In the past 35 years, many of Leighton and Murray's predictions have been verified and demonstrated by measurements taken on Mars (2). However, the existence of a surface reservoir of CO_2 large enough to have important implications for long-term climate and climate stability has yet to be demonstrated (3, 4). Here we report observations, made with the Mars Global

Surveyor (MGS)/Mars Orbiter Camera (MOC), of interannual morphologic changes in the south polar residual cap that support the argument for a climatologically important CO_2 reservoir.

The south polar residual cap exhibits morphologies unique to that location, characterized by irregular to circular pits, remnant mesas, and other landforms, interpreted to have formed by collapse and erosion (5). These features range from a few tens of meters to a few hundreds of meters in scale but display only a few meters of relief (5).

The erosion appears confined to, and highlights the layered nature of, the uppermost materials that make up the cap. The layers are relatively uniform in thickness but display a range in surface expression that appears related to their ability to erode (6). As few as one to as many as six layers crop out at various locations within the cap; not all layers are seen at all locales. On the basis of shadow measurements made during this investigation, each layer is about 3 m thick.

MOC was first used to observe the south polar region at high resolution in July 1999 (7). To search for changes, specific locations within the residual cap were reimaged at the same season and time of day beginning in late July 2001 [starting around heliocentric longitude (L_s) 223°±4° and continuing since then]. In each case, a 2.2 to 3.7 m/pixel image covering a portion of an earlier image was acquired (8). Upon receipt, both the original and new images were processed for analysis (9).

Figure 1 shows good examples of pits, intervening ridges, and isolated mounds that have changed. Diametric measurements, made on 100 features on each of four image pairs, indicate that these pits enlarged or their intervening ridges shrank by about 6 ± 2 m and features smaller than ~6 m across disappeared. In other words, in these examples, nonhorizontal surfaces appear to have retreated by ~3 m. Other areas within the residual cap display different morphologies, and some of these show no detectable change. Preliminary statistics suggest that between 25 and 50% of the escarpments have retreated between 1 and 3 m.

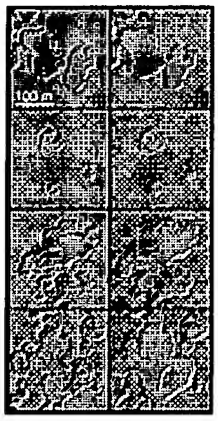

Fig. 1. Pits, intervening ridges, and mounds in south polar residual ice cap. Extracted from orthographically projected, 1 m/pixel versions of M08-04516 (left; 10/19/1999, L_s ~ 227°) and E07-01565 (right; 8/23/2001, L_s ~ 219°). Pit walls and other escarpments have retreated ~ 3 m in one Mars year. Illumination from upper left. [View Larger Version of this Image (84K GIF file)]

As part of the input to an estimate of the total amount of scarp retreat that occurred during the past martian year, the total perimeter in a variety of settings was determined by image processing techniques (10) and divided by the area viewed. Measurements were made on images representative of the range in areal density of various forms of escarpments within the residual south polar cap. The average scarp perimeter per area was 2.4×10^{-2} m/m^{-2}.

We determined that the amount of retreat was consistent with the subliming of a volatile ice by calculating the annual solar insolation using software based on spacecraft navigation routines, and we compared our results with the results of previous models of polar cap behavior (1, 11-13, 14). We used the order of magnitude greater volatility of CO_2 relative to water ice to differentiate between these two candidates. Table 1 summarizes the results of our calculations of the insolation and the equivalent areal mass density for H_2O and CO_2 ice for horizontal surfaces at various latitudes from the equator to near the south pole.

Table 1. Calculated solar insolation and maximum equivalent ice mass erosion for H_2O ice (column 6) and CO_2 ice (column 7) for one martian year on horizontal surfaces at different latitudes (column 1). Columns 2, 3, 4, and 5 give computed solar insolation in energy areal density per Mars year, or its equivalent power density, in several different representative physical units. All four columns present the same information–the solar energy input into the surface, independent of surface material–but in different units. Column 6 was computed using 652 cal/g for the latent heat of H_2O at 145 K. Column 7 was computed using 143 cal/g for the latent heat of CO_2 at 145 K. Values from columns 6 and 7 are used as input to the calculations summarized in Table 2.

	Parameter				Maximum	
					H_2O	CO_2
Latitude	(joules m^{-2} $year^{-1}$)	(W m^{-2})	(cal m^{-2} $year^{-1}$)	(cal cm^{-2} $year^{-1}$)	(g cm^{-2} $year^{-1}$)	(g cm^{-2} $year^{-1}$)
−85°	4.79×10^9	80.7	1.14×10^9	1.14×10^5	175	798
−80°	4.89×10^9	82.3	1.16×10^9	1.16×10^5	178	814
−75°	5.06×10^9	85.2	1.20×10^9	1.20×10^5	185	842
−70°	5.30×10^9	89.4	1.26×10^9	1.26×10^5	194	883
−45°	7.93×10^9	133.6	1.89×10^9	1.89×10^5	289	1320
0°	1.07×10^{10}	179.6	2.54×10^9	2.54×10^5	389	1775

A variety of factors affect the translation of the maximum equivalent areal mass loss (Table 1) to a comparable effective scarp retreat (Table 2), and the result is sensitive to the values assumed for each of these factors. We explored some of these factors and a range of possible values for them (albedos between 0.5 and 0.75 and densities between 1 and 3 g/cm^3). Atmospheric contributions (which can act to enhance or diminish sublimation, depending on seasonal factors), conduction into the surface, and other physical processes that would reduce the amount of energy available for sublimation were represented by an efficiency factor of arbitrary value. We also assumed that slopes of between 30° and 50° (typical of the slopes measured by shadow techniques) facing the equator at 85°S latitude receive roughly the same insolation (with the same efficiency) as horizontal surfaces at 35° to 55°S (this simplification encompasses variations resulting from slope azimuth and season).

Table 2. Calculated amount of ice mass erosion per Mars year for H_2O and CO_2

ice as a function of latitude (column 1) and energy transfer. Columns 2 and 3 show the amount of mass loss per unit area for an albedo of 0.65. Columns 4 through 9 show the equivalent amount of surface retreat for material with a density of 1.5 g/cm and three different efficiencies of energy transfer (100, 50, and 80%). Calculations are for horizontal surfaces; escarpment retreat can be estimated by subtracting the slope declivity for the "actual" latitude to derive an "effective" latitude and reading across the row of that latitude.

Parameter			Efficiency = 100%		Efficiency = 50%		Efficiency = 80%	
	H_2O	CO_2	H_2O	CO_2	H_2O	CO_2	H_2O	CO_2
Latitude	(g cm^{-2} $year^{-1}$)	(g cm^{-2} $year^{-1}$)	(cm $year^{-1}$)	(cm $year^{-1}$)	(cm $year^{-1}$)	(cm $year^{-1}$)	(cm $year^{-1}$)	(cm $year^{-1}$)
−85°	61	279	41	186	20	93	33	149
−80°	62	285	42	190	21	95	33	152
−75°	65	295	43	196	22	98	34	157
−70°	68	309	45	206	23	103	36	165
−45°	101	462	68	308	34	154	54	246
0°	136	621	91	414	45	207	73	331

We first compared our calculations for horizontal surfaces with the areal mass density of CO_2 frost computed using thermal models of the seasonal polar cap near the south pole. From these models, we calculated that between 100 and 150 g/cm^2 is deposited at 80°S latitude each winter and is removed by sublimation each spring and summer (1, 14, 11, 12). When we use parameters similar to those used in these models (albedo = 0.65, density = 1.0 g/cm^3), efficiencies between 35 and 50% reproduce their results; an efficiency of less than 35% permits net accumulation at 80°S, whereas a greater efficiency permits net erosion or the heating of the nonvolatile surface.

For the same assumptions, our calculations suggest that efficiencies between 40 and 80% will lead to 1 to 3 m of retreat of 30° to 50° escarpments in CO_2. More importantly, they show that scarps in water ice could, at most, retreat only a few decimeters. Only extreme combinations of our three parameters (albedo < 0.5, density < 0.5 g/cm^3, and "efficiency" > 80%), which are generally unrealistic, could reproduce in water ice the magnitude of scarp retreat actually observed. We conclude that the erosion is occurring in one or more layers of moderately dense CO_2 ice.

We estimated the amount of material lost from the south polar cap over the past year by mapping the extent of the pitted, layered material (5) on a south polar stereographic map projection of a Mars digital image mosaic, based on close inspection of 144 pre- and immediately postsunrise, 12 to 15 m/pixel survey images acquired during July and August 1999. The map was then transferred to a comparably projected late summer view of the south polar region acquired by the MOC wide angle camera. The extremely strong correlation of the mapped contacts with the albedo of the late summer residual cap in the wide angle image permitted the use of image processing techniques to determine the area of the cap and its pitted surface (~87,000 km^2). The calculated amount of scarp perimeter is ~2 × 10^9 m, and the volume of material lost between 1999 and 2001 is ~2 to 10 × 10^9 m^3 (2 to 10 × 10^{15} cm^3) for the ranges in retreat distance (1 to 3 m) and fraction of

escarpments experiencing retreat (25 to 50%). For densities of CO_2 ice of 1 to 2 g/cm^3, this is 2 to 20 × 10^{15} g, or about 0.008% to 0.08% of the mass of the atmosphere.

A 3 m thick layer of pure CO_2 ice with a density between 1 and 2 g/cm^3 covering the entire residual cap would have a mass of 2 to 4 × 10^{17} g (1 to 2% of the present mass of the martian atmosphere). At a linear recession rate, retreat of the present escarpments would consume a layer in 30 to 150 martian years. However, measurements of the enlargement of different sized pits show that the retreat of escarpments is independent of the size of the pit, so the rate of pit growth and hence release of additional CO_2 into the atmosphere is not linear but will increase with time. For example, the perimeter of a 10-m-diameter pit would double in 2 martian years at a 3 m/year recession rate and at that point would experience twice as much erosion and contribute twice as much gas to the atmosphere as it did 2 years earlier. The size-frequency and areal density relationships for depressions within the polar cap have not been fully quantified, but preliminary values suggest that the erosion of a layer may take only one-third as long as the linear estimate.

Thus, without accounting for deposition elsewhere, this erosion rate implies a secular and increasing contribution of CO_2 into the atmosphere, augmenting its mass by as much as 1% per martian decade. Were sufficient layers of CO_2 available, it would only take a few martian centuries to double the present atmosphere.

We do not know where the CO_2 is going (15). As previously noted (3), thermodynamics favor precipitation of CO_2 in the north polar region, but CO_2 frost is not seen to persist on the northern cap through the summer. The recently released CO_2 probably participates in the formation and retreat of the seasonal frost caps. Where it goes from there is uncertain; as the atmospheric pressure rises, regolith adsorption may increase (16, 17) or CO_2 may be precipitated at locations somewhere in the polar regions not presently detected.

The large, cyclic, and potentially chaotic obliquity and orbital eccentricity variations that Mars is believed to experience as a result of gravitational interactions between the planets may play a role in how, where, and when the surface reservoir forms, but calculations (18-22) show that values for these attributes have not changed substantially over the past 10,000 to 20,000 years. Given the high rates of destruction of the CO_2 layer(s), it is not clear that any of them could be surviving from the last period of dramatically low obliquity (when the polar regions would have been substantially colder) or dramatically high obliquity (when the higher polar temperatures might have been offset by higher atmospheric pressures to permit polar deposition) or from the last period when the polar temperatures were changing rapidly.

Repeated MOC observations indicate that a surface reservoir of solid CO_2 persists year-round on Mars and that this deposit is not in equilibrium with the present polar environment (it is being eroded). The rate and amount of erosion are phenomenal—the amount of scarp retreat, although small on a planetary scale, is substantially greater than any change previously identified on Mars at meter scale (7). It is unlikely that this rate can be sustained indefinitely, because the entire relief beneath the visible portion of the south polar residual cap, were it CO_2, could be sublimed to vapor in a few thousand Mars years. These and other observations (7, 23) suggest that the present martian environment is neither stable nor typical of the past.

REFERENCES AND NOTES

1. R. L. Leighton and B. C. Murray, *Science* **153**, 136 (1966) [Abstract/Free Full Text] .
2. The predicted composition of the seasonal cap was confirmed to be CO_2 by infrared measurement of its temperature in 1969 (24). The predicted pressure variation cycle was confirmed by in situ measurement by the Viking 1 and Viking 2 landers between 1976 and 1982 (25-27).
3. Leighton and Murray (1) posited that the permanent deposit of CO_2 would be found in the north, but this view was shown to arise from an oversimplification in the inputs to their thermal model (28). Other studies (29, 30) suggested that the remnant, nonseasonal frost caps were both water ice, although Murray and Malin (28) argued that the north polar region was favored over the south for retention of CO_2 because at more than a 3 km lower altitude (31) (now known to be more than 6 km) (32) (and hence higher pressure), the CO_2 frost point was at an appreciably higher temperature (almost 6 K higher) (33). Calculations show that deposits of CO_2 arbitrarily introduced at the south pole migrate north rapidly (14). Viking orbiter infrared observations demonstrated that the north polar residual cap was indeed water ice but that the south polar residual cap was CO_2 (34-36). The presence of the CO_2 cap in the south, despite the argument raised by Murray and Malin (14, 28, 33), was explained by the extreme sensitivity of the equilibrium temperature to albedo; the south polar cap is more than 30% brighter in the spring than is the comparable northern cap (37), an effect attributed to northern winter deposition of dust raised each year during the period of most intense dust storm activity (southern summer) (38), which leads to "dirtier" frost and hence lower albedo in the north.
4. Although there is broad consensus that the southern residual cap is CO_2, the general impression from the literature is that the material is thin and occasionally may completely sublime. The only evidence put forth for this variability is the ground-based detection of abundant water vapor during the 1969 southern summer (39), an observation that would be at odds with the presence of CO_2 ice upon which the atmospheric water vapor would tend to deposit. The Viking orbiters observed only trace amounts of water vapor in 1977 (40), as would be expected in the presence of year-round CO_2 ice, and an analysis of Mariner 9 infrared measurements indicated that the southern residual cap in 1971 and 1972 also retained CO_2 frost throughout the summer (41). These inconsistent observations have been taken as evidence of an interannual instability (42) and have been used to argue that Leighton and Murray's prediction of a large surface reservoir is wrong (42) or that as yet unknown feedback processes between the other CO_2 reservoirs (atmosphere, polar cap, carbonate rocks, and gas adsorbed onto fine-grained regolith materials) maintain the near-zero mass of the surface frost (41).
5. P. C. Thomas, *et al.*, *Nature* **404**, 161 (2000) [CrossRef] [ISI] [Medline] .
6. Factors that may affect the erosion of the polar cap surface are the magnitude and orientation of regional slope, proximity to features with large (>100 m) local relief, density of the frost deposit, abundance and nature of nonvolatile components within the materials, and surface albedo and texture.
7. M. C. Malin, K. S. Edgett, *J. Geophys. Res.* **106**, 23,429 (2001).
8. MOC is a line-scan camera that acquires images one line at a time (similar to a flatbed scanner or facsimile machine) (43, 44). With about 80 Mbits of buffer space, a losslessly compressed, full-resolution (~ 1.5 m/pixel) image 3 km across can be at most only 12 km in length. Positional uncertainties predicted several days in advance (the length of time it takes to acquire and process tracking data, examine the predicted orbit ground tracks for targets, and generate and transmit commands to the instrument to image those targets) vary from 3 to 9 km. By summing images by two, MOC images can cover these

uncertainties for more than one polar image per orbit, at the expense of resolution (3 m/pixel).

9. Images were first radiometrically calibrated to remove instrument signature. They were then digitally warped to an orthographic projection with a common pole on the International Astronomical Union defined reference spheroid with spacecraft position reconstructed from tracking and attitude information determined by the onboard attitude control and articulation subsystem. The images were projected to a scale of 1 m/pixel. To reduce the impact on image comparison of small, cyclic roll oscillations that differentially displace features observed in two line-scan images, we additionally registered the orthographic projections by warping the images to a set of tiepoints. Additional cosmetic processing was applied to enhance features.
10. This processing took advantage of the sharp demarcation of slopes in the low-Sun elevation images. Processing involved a combination of thresholding to increase the contrast of slopes to the surrounding horizontal surfaces, gradient amplification to isolate the slopes from the horizontal surfaces, and erosion to replace each slope with a single line. Histograms provided the integrated perimeter length and image area.
11. G. A. Briggs, *Icarus* **93**, 167 (1974) [CrossRef].
12. O. B. Toon, *et al.*, *Icarus* **44**, 552 (1980) [CrossRef] [ISI].
13. D. A. Paige and K. D. Keegan, *J. Geophys. Res.* **99**, 25993 (1994) [CrossRef] [ISI].
14. W. R. Ward, *et al.*, *J. Geophys Res.* **79**, 3387 (1974) [ISI].
15. Present data do not suggest that deposition is occurring someplace else in the south polar region. About 25% of the south polar residual cap has been imaged at better than 4 m/pixel. Much of this coverage is not contiguous, so the sampling of the polar cap is good. No morphological indications of deposition are seen adjacent to escarpments or in flat interscarp areas.
16. F. P. Fanale and W. A. Cannon, *J. Geophys. Res.* **79**, 3397 (1974) [ISI].
17. F. P. Fanale, *Icarus* **28**, 172 (1976) .
18. B. C. Murray, *et al.*, *Science* **180**, 638 (1973) [Abstract/Free Full Text] .
19. W. R. Ward, *Science* **181**, 260 (1973) [Abstract/Free Full Text] .
20. W. R. Ward, *J. Geophys. Res.* **79**, 3375 (1974) [ISI].
21. J. Touma and J. Wisdom, *Science* **259**, 1294 (1993) [Abstract/Free Full Text] .
22. J. Laskar and P. Robutel, *Nature* **361**, 608 (1993) [CrossRef] [ISI] .
23. M. C. Malin and K. S. Edgett, *Science* **288**, 2330 (2000) [Abstract/Free Full Text] .
24. G. Neugebauer, *et al.*, *Astron. J.* **79**, 719 (1971) [CrossRef].
25. S. L. Hess, *et al.*, *Science* **194**, 78 (1976) [Abstract/Free Full Text] .
26. S. L. Hess, *et al.*, *Science* **194**, 1352 (1976) [Abstract/Free Full Text] .
27. S. L. Hess, *et al.*, *J. Geophys. Res.* **82**, 4559 (1977) .
28. B. C. Murray and M. C. Malin, *Science* **182**, 437 (1973) [Abstract/Free Full Text] .
29. B. C. Murray *et al.*, *Icarus* **17**, 328 (1972).
30. L. A. Soderblom, *et al.*, *J. Geophys. Res.* **78**, 4197 (1973) [ISI].
31. D. Dzurisin and K. R. Blasius, *J. Geophys. Res.* **80**, 3286 (1975) [ISI].
32. D. E. Smith, *et al.*, *Science* **284**, 1495 (1999) [Abstract/Free Full Text] .
33. S. M. Clifford, *et al.*, *Icarus* **144**, 210 (2000) [CrossRef] [ISI] [Medline].
34. H. H. Kieffer, *et al.*, *Science* **194**, 1341 (1976) [Abstract/Free Full Text] .
35. H. H. Kieffer, *et al.*, *J. Geophys. Res.* **82**, 4249 (1977) .
36. H. H. Kieffer, *J. Geophys. Res.* **84**, 8263 (1979) [ISI].
37. D. A. Paige and A. P. Ingersoll, *Science* **228**, 1160 (1985) [Abstract/Free Full Text] .

38. R. W. Zurek, *Icarus* **50**, 288 (1982) [CrossRef] [ISI].
39. B. M. Jakosky and E. S. Barker, *Icarus* **57**, 322 (1984) [CrossRef] [ISI].
40. C. B. Farmer and P. E. Doms, *J. Geophys. Res.* **84**, 2881 (1979) [ISI].
41. D. A. Paige, *et al.*, *J. Geophys. Res.* **95**, 1319 (1990) [ISI].
42. B. M. Jakosky and R. M. Haberle, *J. Geophys. Res.* **95**, 1359 (1990) [ISI].
43. M. C. Malin, *et al.*, *Int. J. Imaging Sys. Technol.* **3**, 76 (1991) .
44. M. C. Malin, *et al.*, *J. Geophys. Res.* **97**, 7699 (1992) [ISI].
45. We acknowledge the significant contribution to this work made by the MGS/MOC operations teams at Malin Space Science Systems, the Jet Propulsion Laboratory (JPL), and Lockheed Martin Astronautics. M. C. M. acknowledges the role of B. C. Murray in challenging, stimulating, and leading three generations of investigators of the martian polar regions. This work benefited greatly from discussions with K. S. Edgett. Supported under JPL contract numbers 959060 and 200780.

20 August 2001; accepted 11 October 2001
Published online 1 November 2001; 10.1126/science.1066416
Include this information when citing this paper.